

CHAPTER 56

FREAK WAVES IN UNIDIRECTIONAL WAVE TRAINS AND THEIR PROPERTIES

Takashi YASUDA* , Nobuhito MORI** and Kazunori ITO†

ABSTRACT

This study aims to make clear the cause and occurrence condition of two-dimensional(2-D) freak waves by solving the hydrodynamic equations of 2-D irrotational flow for nonlinear waves with various spectra corresponding to swell from wind waves and describing the long-time evolution. As a result, it is shown that the third order resonant interaction causes the 2-D freak waves of which surface profiles are very similar with those observed in nature and multiplies the occurrence probability with the decreasing of the spectral bandwidth in deep water. Conversely, the feature of the freak waves —*single and outstanding wave height*— gets prominent with the broadening of the spectral bandwidth.

INTRODUCTION

In recent years there has been a growing interest in single extreme waves referred as freak waves. Freak waves are individual high waves having severely damaging potential and are defined as waves with larger heights than two times of significant wave heights. There is no doubt on the occurrence of freak waves in nature because many reports are presented on their damages on offshore platforms at deck level and so on. However, the cause and properties of freak waves are still not so clear, although the state of the research on freak waves is already summarized at NATO Advanced Research Workshop in 1989[Peregrine,1990] and some explanations are suggested as their possible cause.

Laboratory measurement(Stansberg,1990) showed that a freak wave can be generated in a 2-D wave flume. This is a fairly strong evidence showing that some freak waves can actually occur in a unidirectional wave train without the effects of directional contents, wave focusing and currents. However, so definite explanation has not yet been suggested for its occurrence. In the case of

*Prof., Dept. of Civil Engineering, Gifu Univ., 1-1 Yanagido, Gifu 501-11, Japan

**Graduate Student, Dept. of Civil Engineering, Gifu Univ., 1-1 Yanagido, Gifu 501-11, Japan

†Research Engineer, Technology Research Center, Taisei Corporation, 344-1 Nasemachi, Totsuka-ku, Yokohama, Kanagawa 245, Japan

a quasi-monochromatic wave, Dold & Peregrine(1986) solved the fully nonlinear hydrodynamic equations for 2-D irrotational waves by using a boundary integral method and showed that a unidirectional wave train as gentle as $ka=0.10$ undergoes a considerable modulation in its envelope and develops into breaking due to the nonlinear modulation. Their result suggests that the modulation due to resonant interaction might generate a freak wave in the 2-D domain. However, even if freak waves in nature could be treated approximately as long crested(2-D) waves, it remains unchanged that they must be treated as random waves having considerably broad spectral bandwidth. We hence are required to answer the question whether or not the resonant interaction can actually generate such freak waves as observed in nature in the 2-D wave trains having the broad band spectra similar with those in field.

In this study, we focus our interest on 2-D freak waves and make clear their cause and occurrence condition. For that purpose, we solve the hydrodynamic equations of 2-D incompressible and inviscid fluid for the waves having various spectra from swell to wind waves and perform intensive numerical simulations describing their long-time evolution. On the basis of the simulated results, we investigate relationships between their initial conditions and the time evolution and give an answer to the question whether or not 2-D freak waves can actually occur in random wave trains with arbitrary spectra. Furthermore, we make clear their cause and occurrence condition.

COMPUTATIONAL METHOD

2-D vertical domain is assigned to be the usual spatial coordinates(x, z);the origin is located at the mean water level, x the horizontal coordinate and z the vertically upward one. Boundary conditions at the free surface of the irrotational flow are rewritten into the evolution equations with regard to the free surface profile $\eta(x, t)$ and the surface velocity potential $\phi^s(x, t)$ at $z = \eta$;

$$\eta_t + \phi_x^s \cdot \eta_x - (1 + \eta_x \cdot \eta_x) \phi_z = 0 \Big|_{z=\eta}, \quad (1)$$

$$\phi_x^s + g\eta + \frac{1}{2} \phi_x^s \cdot \phi_x^s - \frac{1}{2} (1 + \eta_x \cdot \eta_x) \phi_z^2 = 0 \Big|_{z=\eta}, \quad (2)$$

where the subscripts denote the partial differentiations with regard to t and x , ϕ_z the vertical gradient of the velocity potential $\phi(x, z, t)$, t the time and g the acceleration due to gravity.

It is very difficult to solve eqs.(1) and (2) into the so-called Zakharov equation on the wavenumber space for waves having both the nonlinearity higher than the 3rd order and the arbitrary spectral bandwidth as far as based on the ability of present computer, although it was carried out for quasi-monochromatic waves by Yuen & Lake(1982). Hence, following Dommermuth & Yue(1987), we solve eqs.(1) and (2) on the physical space. Considering the nonlinear correction to ϕ_z up to the M th order in the wave field composed of J-Fourier modes, we

formulate ϕ_z so as to satisfy the Laplace equation, $\nabla^2 \phi = 0$, and the boundary condition on the flat bottom at $z=-h$, $\phi_z=0|_{z=-h}$;

$$\phi_z(x, \eta, t) = \sum_{m=1}^M \sum_{k=0}^{M-m} \frac{\eta^k}{k!} \sum_{j=1}^J \phi_j^{(m)}(t) \frac{\partial^{k+1}}{\partial z^{k+1}} \psi_j(x, 0), \tag{3}$$

$$\psi_j(x, z) = \frac{\cosh[k_j(z+h)]}{\cosh(k_j h)} \exp(ik_j x), \tag{4}$$

where k denotes the wave number, h the mean water depth, $\phi_j^{(m)}(t)$ is derived by solving the following equations in order.

$$\begin{aligned} \phi^{(1)}(x, 0, t) &= \phi^s, \\ \phi^{(m)}(x, 0, t) &= - \sum_{k=1}^{m-1} \frac{\eta^k}{k!} \frac{\partial^k}{\partial z^k} \phi^{(m-k)}(x, 0, t) \quad (m = 2, 3, \dots, M). \end{aligned} \tag{5}$$

In this method, an approximation is made on the expression of ϕ_z alone and eqs.(1) and (2) are solved directly in the physical space by using the pseudo-spectral method. While the spatial derivations of $\phi^{(m)}$, ϕ^s and η are evaluated in the spectral space, the nonlinear products are calculated in the physical space. The time evolution of η and ϕ^s is made in the physical space by integrating eqs.(1) and (2) with the fourth-order Runge-Kutta-Gill method. An optimum FFT scheme for the vector operation in a super computer is used to delete the alising error generated in the computaion of the nonlinear terms and accomplish the fast computation.

VALIDITY OF THE COMPUTATION

The accuracy and convergence of the computational model are tested by giving the exact Stokes waves as initial waves. The first check of the accuracy is provided by examining the maximum difference of the surface wave profile $\varepsilon_1 = |k\{\eta_n(x, t) - \eta_e(x, t)\}|_{max}$ between the numerical solution η_n and the exact solution η_e during the propagation process from $t/T=0$ to 100. Here, T is the wave period. Further, the accuracy and convergence of the numerical solutions are tested by defining the error to the conservation law of the total energy $E(t)$ as $\varepsilon_2 = |1 - E(t)/E(0)|$ and examining its time evolution.

Table 1 indicates the maximum values of ε_1 and ε_2 for the shallow water waves with $ka=0.17$ and $kh=1$ and for the deep water waves with $ka=0.2$ and 0.3 when the numerical computations are made under the condition of the values of $M=3$ and 4 and $J=8$ and 16 . Here, a is the wave amplitude. Figure 1 describes the time evolution of ε_2 for each numerical solution shown in Table 1. Both the error criteria, ε_1 and ε_2 , indicate finite values because the values of M and J employed here are not large enough for the numerical solutions to agree completely with the exact solution. However, the values of ε_1 are still considerably

small after the long time evolution of $t/T=100$. Further, although the values of ϵ_2 grow with oscillation, their envelopes are almost constant independly of the values of kh, ka, M and J and their amplitudes are sufficently small. We can hence expect the sufficient accuracy and convergency for the obtained numerical solutions if solving eqs.(1) and (2) by the aforementioned method.

Table 1. Accuracy of the numerical solutions for the exact Stokes waves

ka	kh	M	J	$\epsilon_1 \times 10^3$	$\epsilon_2 \times 10^3$
0.17	1	3	8	0.43	1.33
0.17	1	4	8	0.37	0.85
0.20	∞	3	8	0.42	0.72
0.20	∞	3	16	0.42	0.72
0.20	∞	4	8	0.42	0.70
0.30	∞	3	8	3.05	5.75

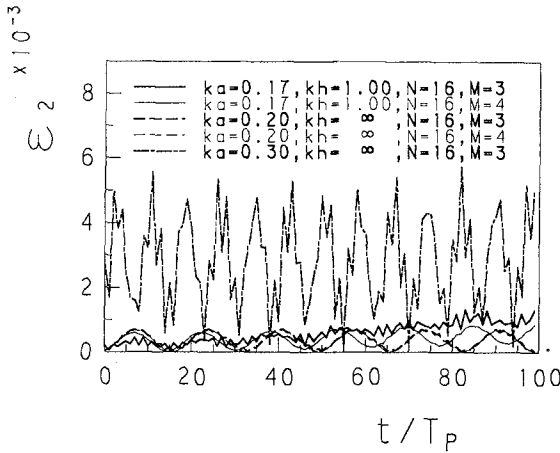


Figure 1. Time histories of the error criterion ϵ_2

NUMERICAL SIMULATIONS

Initial surface profiles $\eta(x, 0)$ is given by

$$\eta(x, 0) = \sum_{n=1}^J \sqrt{2S(k_n)(2\pi/L_0)} \sin(k_n x + \epsilon_n) \tag{6}$$

where L_0 is the total length of the simulated wave train, k_n the wave number of the n -th Fourier mode, ϵ_n the phase constant of the Fourier mode given by a set of independent uniform random numbers uniformly distributed in the interval $(0, 2\pi)$ radians and $S(k_n)$ the desired wavenumber discrete spectrum into which the following Wallops continuous spectrum $S(f)$ is transformed through the linear dispersion relation.

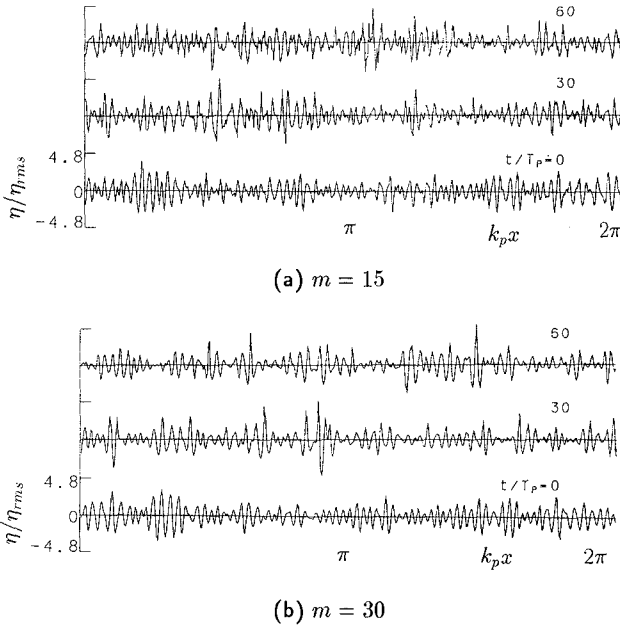


Figure 2. Spatial surface profiles of a simulated wave train at $t/T_p=0, 30$ and 60 ($k_p h=3.0, k_p a=0.17$).

$$S(f) = \alpha H_{1/3}^2 f^{(4-m)} (f/f_p)^{-4} \exp \left[-0.25m (f/f_p)^{-4} \right], \tag{7}$$

where α is a constant satisfying the relation,

$$H_{1/3} = 4.004 \left[\int_0^\infty S(f) df \right]^{\frac{1}{2}}, \tag{8}$$

f_p the spectral peak frequency, $H_{1/3}$ the significant wave height and m the spectral bandwidth parameter. The value of $m=5$ generally gives the spectrum of wind waves and those of $m \geq 10$ swell spectra. Initial surface potential $\phi^s(x, 0)$ is given here by the linear transformation of its conjugate $\eta(x, 0)$.

The numerical computations are made in the periodic space having the length of $L_0 = 64L_p$ on the x coordinate; the subscript p denotes the quantity of the spectral peak mode. The values of M and J are fixed to 3 and 256, respectively. The time interval of the stepping is $T_p/100$. The simulations are performed with the accuracy of the energy error criterion ε_2 of which value is always less than 0.05, under the initial statistics comprised of $k_p h=1.04, 1.36, 1.72, 2.35$ and $3.0, k_p a=0.17, m=5, 10, 15$ and 30 . The accuracy is accomplished without any consideration except for de-aliasing. This fact convinces us that

any breaking event does not occur during the propagation process because the breaking triggers the floating overflow error of the numerical solution.

Figure 2 shows the computed surface elevations for the waves with the initial statistics of $k_p h = 3.0$, $k_p a = 0.17$ and $m = 15, 30$. The free surface elevations at $t/T_p = 20$ and 60 are considerably modulated in comparison with their initial ones and accompany single high waves characterized as freak waves because they are not part of a smooth wave group pattern and the crest heights clearly exceed those of their neighbours.

NONLINEAR EFFECTS ON 2-D FREAK WAVES

Surface profiles of 2-D freak waves

Figure 3 shows the temporal surface elevation of the typical freak wave observed in the North sea (Sandet *al.*, 1990). The wave profile definitely demonstrates the feature of a typical freak wave that is single —*not part of smooth wave group pattern*— and has remarkable horizontal asymmetry and the crest height clearly exceeding that of its neighbours.

Figure 4 indicates the spatial surface profiles of 2-D freak waves occurring in the simulated wave trains. The simulated wave profiles are easily found to be very similar with the observed wave profile shown in Fig. 3, although there is a definite difference that the formers are spatial profiles in 2-D domain while the latter is temporal one in 3-D field. On the other hand, the wave profile of a linear freak wave shown in Fig. 5 for comparison is mild and horizontally symmetric. We thereby notice that it is greatly differs from those shown in Figs. 3 and 4 and very little possesses the aforementioned feature of the freak waves. This states that a linear combination of the Fourier modes cannot be probably the cause of the freak waves hitherto observed in nature even if it can generate the wave grouping containing a high wave of which height exceeds two times of $H_{1/3}$. On the contrary, the wave profiles shown in Fig. 4 are very similar with that observed in nature (Fig. 3) as mentioned. We could therefore say from the viewpoint of the similarity of both the wave profiles that freak waves can be generated by the 3rd order nonlinear interaction (resonant interaction) independently of the spectral bandwidth, that is, the 3rd order resonant interaction can be one of the causes of freak waves in nature. We should further notice that even if the occurrence of the freak waves might obey the Rayleigh distribution, which is based on the strict assumption of a narrow banded Gaussian process, the freak waves having the aforementioned feature —*single and outstanding*— never occurs from narrow banded linear wave trains.

Figure 6 describes the time evolution of the freak wave during the propagation process from its appearing to disappearing. Its appearing and disappearing times are denoted with the open arrows. The freak wave is not so unstable as it instantaneously appears and disappears, but so stable as it keeps the profile during about one period at least.

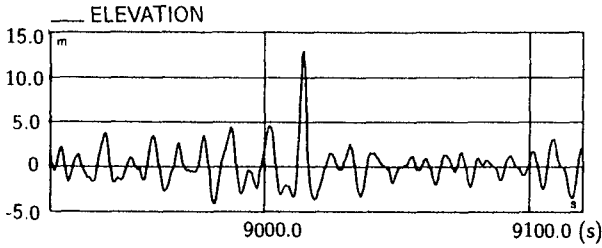
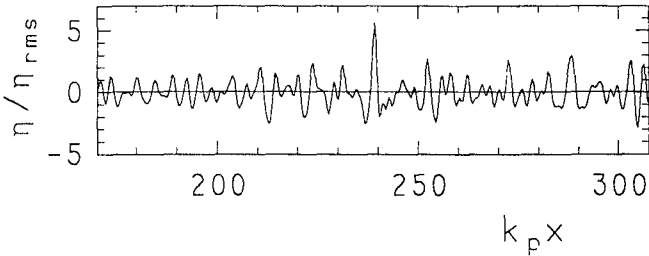
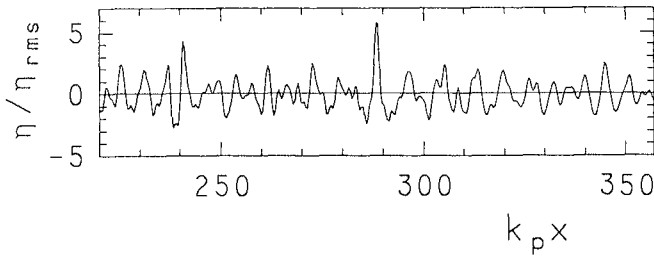


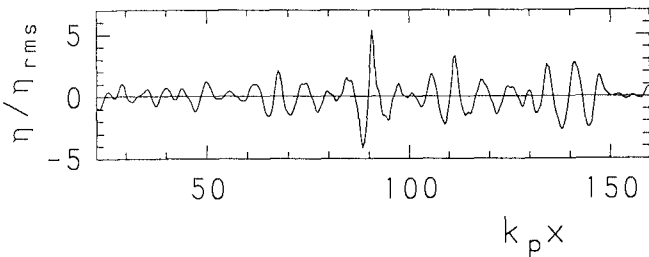
Figure 3. Temporal surface elevation of the freak wave observed in the North sea [Sand et al., 1990].



(a) $m = 5$



(b) $m = 15$



(c) $m = 30$

Figure 4. Spatial surface profiles of the freak waves occurring in the simulated 2-D nonlinear wave trains ($k_p h = 3.0, k_p a = 0.17$).

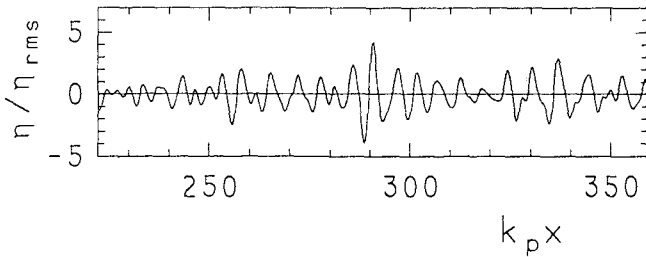
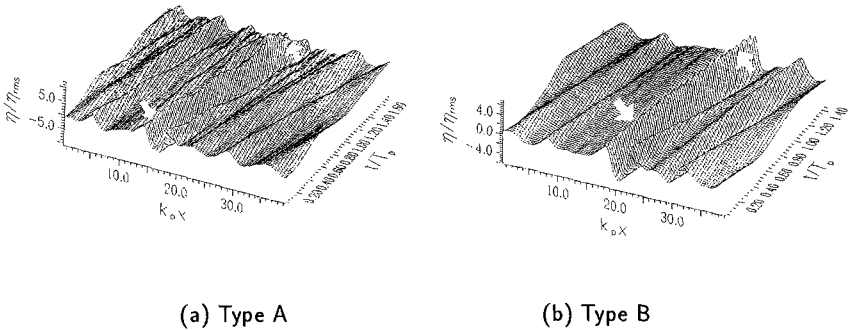


Figure 5. Spatial surface profile of a linear freak wave which occurs in a 2-D linear wave train($k_p h=3.0, k_p a=0.17, m=15$).



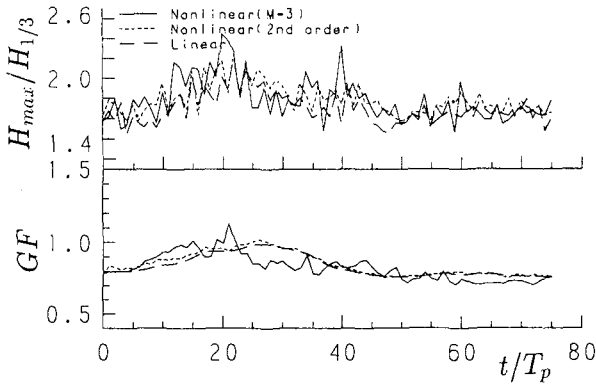
(a) Type A (b) Type B
 Figure 6. Propagation process of the 2-D freak wave from its appearing to disappearing($k_p h=3.0, k_p a=0.17, m = 30$).

Nonlinear effects causing freak waves

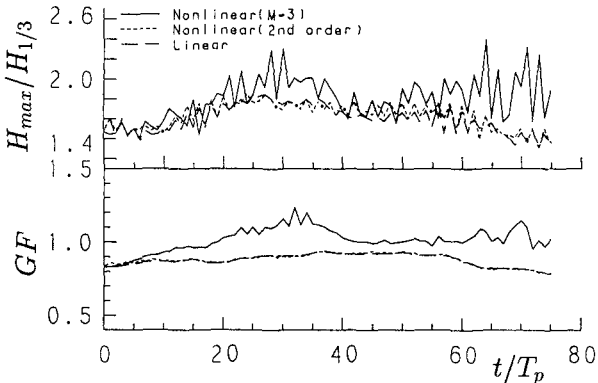
Figure 7 shows the time histories of the ratio $H_{max}/H_{1/3}$ of the maximum wave height H_{max} to $H_{1/3}$ and GF (Groupiness Factor) of the spatial surface profiles of the evolving simulated waves. For comparison, the results of linear waves and the 2nd order nonlinear waves are also shown. The 2nd order nonlinear wave solution is derived by solving not eqs.(1) and (2) but the original hydrodynamic equations in which the nonlinear terms more than the 3rd order are deleted. The 3rd order resonant interaction is not therefore taken into account in the 2nd order solution. It is found that nonlinear effects of the 2nd order are almost negligible on the values of $H_{max}/H_{1/3}$ and GF , although it is well-known that they affects on the skewness of the free surface profiles. On the other hand, nonlinear effects of the 3rd order on those values are remarkable and grow with the narrowing of the spectral bandwidth. The time evolution of $H_{max}/H_{1/3}$ corresponds well to

that of GF in the nonlinear($M=3$) wave train. We could hence say that the 3rd order resonant interaction strongly modulates the envelope of the wave train so that it multiplies the values of GF and H_{max} and further causes the freak waves.

Figure 8 shows the amplitude modulation of the peak and its side-band Fourier modes of the nonlinear waves($M=3$) shown in Fig.7. The time evolution of the amplitude modulation of the side-band modes clearly corresponds to both the time histories of $H_{max}/H_{1/3}$ and GF . It should be noticed that the value of $H_{max}/H_{1/3}$ exceeds 2 and the individual wave with H_{max} becomes a freak wave at the time when the side-band modes become dominant to the spectral peak mode independently of the spectral bandwidth($m=15$ and 30) and that these occur. This result demonstrates that the 2-D freak waves are generated by the side-band instability due to the resonant interaction.



(a) $m = 15$



(b) $m = 30$

Figure 7. Time histories of $H_{max}/H_{1/3}$ and GF for the evolving nonlinear wave trains($M=3$ and the 2nd order) and the linear one($k_p h=3.0, k_p a=0.17$).

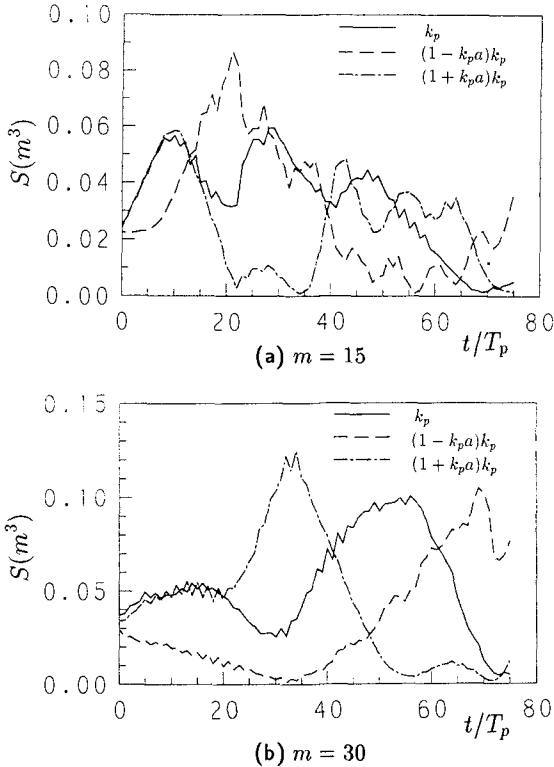


Figure 8. Time evolution of the modal energy $S(k)$ of the spectral peak mode(k_p) and its both side-band modes($k_p \pm k_p^2 a_{1/3}$) of the nonlinear waves($M=3$) corresponding to the case reported in Fig.7($k_p h=3.0, k_p a=0.17$).

Nonlinear effects on the occurrence probability

Figure 9 compares the frequency distribution of $H_{max}/H_{1/3}$ obtained from the spatial surface profiles at every time step of $\Delta t/T_p=1$ of the simulated waves during the propagation process from $t/T_p=0$ to $t/T_p=75$ with the following distribution $p(H_{max}/H_{1/3})$ derived from the Rayleigh distribution,

$$p(x_{max}) = 2.832x_{max}\xi \exp(-\xi), \tag{9}$$

where $x_{max}=H_{max}/H_{1/3}$, $\xi=N \exp(-1.416x_{max}^2)$. N_{min} and N_{max} in the Fig.9 denote the minimum value and the maximum one of the number of the zero-down crossing waves contained in the simulated waves during the propagation process. The frequency in the 2nd order nonlinear waves is not so influenced by the spectral bandwidth and is presumed to be almost same with that in linear waves because the 2nd order nonlinear interaction very little influences on the

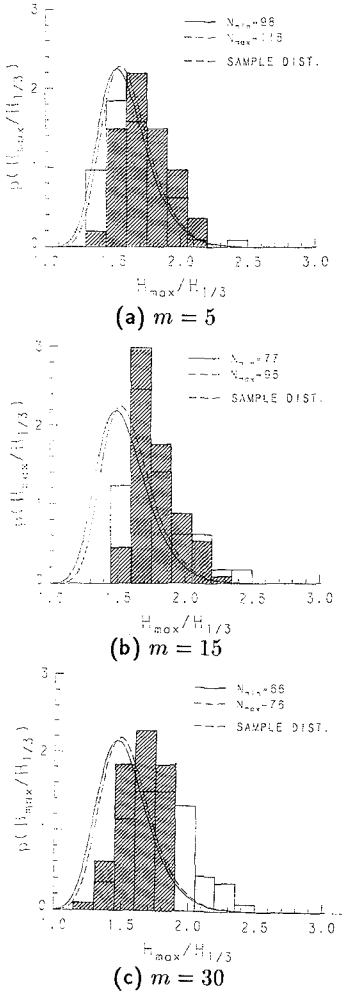


Fig.9. Effects of the nonlinear interaction and spectral bandwidth on the frequency distribution of $H_{max}/H_{1/3}$

On the contrary, the value of μ in the nonlinear wave train largely exceeds that given by eq.(10) independently of the number of N . This suggests that the resonant interaction increases the occurrence probability of the 2-D freak waves 10 times ($N=70$) from 5 times ($N=500$) of that given by eq.(10).

wave height as mentioned above. The difference between both the frequencies (2nd and $M=3$) thereby indicates the influence of the 3rd order resonant interaction on the frequency. It could hence be found from the difference that the influence of the resonant interaction is almost negligible in the case of $m=5$ but becomes non-ignorable over the region of $m \geq 15$. We could thus say that the effects of the resonant interaction become pronounced and the occurrence probability of the freak waves accordingly increases as the spectral bandwidth becomes narrower.

Further, in order to investigate the influence of the number N of the zero-crossing waves on the exceedance probability μ that the value of $H_{max}/H_{1/3}$ is exceeds 2, that is, the occurrence probability of the 2-D freak waves, we compare the value of μ obtained from the simulated wave train ($M=3$) with that given by

$$\mu = 1 - \exp(-N/3041), \quad (10)$$

which is derived under the assumption that N -wave heights obey the Rayleigh distribution. The result is shown in Fig.10 for the waves with the number N of the zero-down crossing waves contained in the initial waves, 70, 150 and 500, respectively. The value of μ in a linear wave train shown for comparison corresponds well to the solid line given by eq.(10) and the difference between both the results could be regarded to be within the region of statistical variation.

Figure 11 shows the relation between the frequency that the value of $H_{max}/H_{1/3}$ of the simulated waves ($M=3$) exceed 2 during their propagation process and the value of GF averaged over the propagation process, $\langle GF \rangle$. Symbols drawn with thick line indicate the values of the waves of which initial bandwidth parameter m equals to 30, those drawn with median line indicate the values with the initial statistics of $m=15$ and those drawn with thin line denote the values with $m=5$. The mean number $\langle N \rangle$ of the zero-down crossing waves in this case is about 80~100, so that if those wave heights obey the Rayleigh distribution, the theoretical value of $p(H_{max}/H_{1/3} > 2)$ is about 0.026.

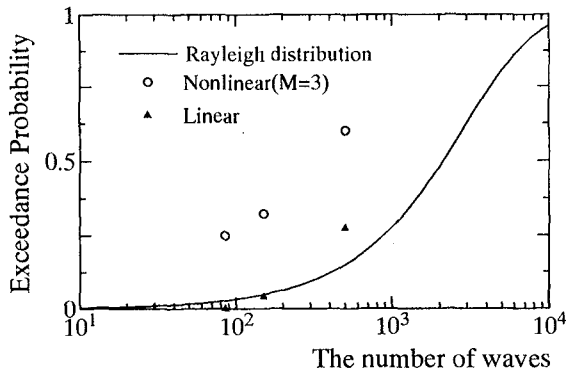


Figure 10. Influence of the number N of the zero-down crossing waves on the exceedance probability $\mu(H/H_{1/3} > 2)$ [$k_p h = 3.0, k_p a = 0.17, m = 30$]

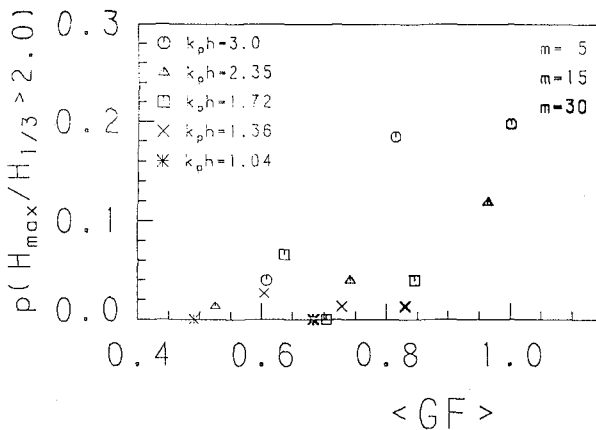


Figure 11. Relation of the occurrence probability of the 2-D freak wave during the propagation process and the averaged value of GF over the process.

Table 2 Relations of the initial statistics to the frequencies(%) of $H_{max}/H_{1/3} > 2$, $\kappa > 2$ and $\chi > 0.65$.

m		$k_p h$		
		3.0	1.72	1.04
5	$H_{max}/H_{1/3} > 2$	6.6 (1.3)	2.6(9.2)	0.0 (0.0)
	$\kappa > 2$	23.7(14.5)	5.2(7.9)	18.4(19.7)
	$\chi > 0.65$	19.7 (1.3)	11.8(5.3)	5.2 (1.3)
		2.6 (0.0)	0.0(0.0)	0.0 (0.0)
15	$H_{max}/H_{1/3} > 2$	22.3 (5.2)	1.3(0.0)	0.0 (1.3)
	$\kappa > 2$	34.2 (0.0)	19.7(7.9)	2.6 (0.0)
	$\chi > 0.65$	14.5 (0.0)	17.1(1.3)	7.8 (0.0)
		1.3 (0.0)	0.0(0.0)	0.0 (0.0)
30	$H_{max}/H_{1/3} > 2$	23.7 (0.0)	2.6(0.0)	0.0 (0.0)
	$\kappa > 2$	19.7 (0.0)	6.6(0.0)	0.0 (0.0)
	$\chi > 0.65$	13.2 (0.0)	9.2(0.0)	7.9 (0.0)
		0.0 (0.0)	0.0(0.0)	0.0 (0.0)

Although the value of $p(H_{max}/H_{1/3} > 2)$, that is, the occurrence probability of the freak wave is independent of the value $\langle GF \rangle$ in the waves with the value of $k_p h$ less than 1.72, the occurrence probability is multiplied with the increasing of the value of $\langle GF \rangle$ in the waves with the value of $k_p h$ over 2.35.

Following Klinting & Sand(1987), we calculate the frequencies that the ratio $\kappa(=H_{i+1}/H_i)$ of the wave height to its neighbour exceeds 2 and that the ratio $\chi(=\eta_{max}/H_{max})$ of the crest height η_{max} to the maximum wave height H_{max} exceeds 0.65, in addition to the frequency of $H_{max}/H_{1/3} > 2$ and show the values of these frequencies to each initial statistics in Table 2. The numerical values on the fourth line the case of $k_p h=3.0$ within the frame corresponding to each wave indicate the frequency satisfying simultaneously these three conditions, $H_{max}/H_{1/3} > 2$, $\kappa > 2$ and $\chi > 0.65$. The figures in parentheses indicate the values in linear waves with the same initial statistics. The frequency of $H_{max}/H_{1/3} > 2$ increases as the spectral bandwidth gets to narrower. On the contrary, the conditions characterizing the freak waves, that is, the frequencies of $\kappa > 2$ and $\chi > 0.65$ increase large as the spectral bandwidth gets to narrower. We could hence say that the 2-D freak waves incline to occur in deep water because their cause —*resonant interaction*— is strengthened to the maximum extent in deep water. Furthermore, it should be noted that although the occurrence probability itself of freak waves defined by $H_{max}/H_{1/3} > 2$ increase with the decreasing of the spectral bandwidth, the occurrence probability of the typical freak waves possessing the feature —*single and the crest height clearly exceed those of its neighbour*— with the increasing of the spectral bandwidth and becomes maximum under the broad band spectra corresponding to wind waves.

CONCLUSIONS

The following major conclusions may be drawn from this study

- i) The 3rd order resonant interaction causes single extreme high waves typically characterized as freak waves in unidirectional wave trains with various spectra corresponding to wind waves from swell. On the other hand, the surface profile of a linear freak wave caused by a linear combination of the Fourier modes is mild and horizontally symmetric and is very different from those observed in nature. Since the resonant interaction is thus essential to cause the 2-D freak waves, its effects on the occurrence probability of the 2-D freak waves should be taken into account.
- ii) The resonant interaction multiplies the occurrence probability of the 2-D freak waves and its effects become pronounced as the water depth gets deeper and the spectral bandwidth gets narrower. However, the feature of the surface profile characterizing freak waves —*single, remarkably horizontal asymmetric and extreme high waves*— gets prominent with the broadening of the spectral bandwidth, that is, the feature is strengthened to the maximum extent under wind wave spectra in deep water.

REFERENCES

- ◇ Dold, J.W. & D.H. Peregrine (1986), *Wave-wave modulation, Proc.20th Conf.on Coastal Eng.*, Vol.I, pp.163-175 .
- ◇ Dommermuth, D.G. & D.K.P. Yue (1987), *A high-order spectral method for the study of nonlinear gravity waves, JFM.*, Vol.184, pp.267-288 .
- ◇ Klinting, P. & S. Sand (1987), *Analysis of prototype freak waves, in Coastal Hydrodynamics*(ed.R.A.Dalrymple,ASCE), pp.618-632 .
- ◇ Sand, S.*et al* (1990), *Freak wave kinematics, in Water Wave Kinematics*(Eds. A.Tørum & O.T.Gudmestad,Kluwer Academic Pub.),pp.535-549 .
- ◇ Peregrine, D.H. (1990), *Report from the working group on breaking and freak waves, in Water Wave Kinematics* (Eds. A.Tørum & O.T.Gudmestad, Kluwer Academic Pub.),pp.17-20 .
- ◇ Stansberg, C.T. (1990), *Extreme waves in laboratory generated irregular wave trains, in Water Wave Kinematics*(Eds. A.Tørum & O.T.Gudmestad, Kluwer Academic Pub.), pp.573-589 .
- ◇ Yuen, H.C. & B.M. Lake (1982), *Nonlinear dynamics of deep-water gravity waves, Advances in Applied Mechanics*vol.22, pp.67-229 .